Aging and Disease
www.aginganddisease.org
Early access date: October 9, 2026
http://dx.doi.org/10.14336/AD.2026.0702

Original Article

GDF15 Induces Weight Loss with Diet- and Age-Dependent Metabolic Effects Across Tissues in Mice

Laura Salmón-Gómez[1,2,3,4], Victoria Catalán[1,2,3,4], Beatriz Ramírez[1,2,3,4], Maite Aguas-Ayesa[2,4,5], Amaia Rodríguez[1,2,3,4], Sara Becerril[1,2,3,4], Gema Frühbeck[1,2,3,4,5], Javier Gómez-Ambrosi[1,2,3,4*]

[1]Metabolic Research Laboratory, Clínica Universidad de Navarra, Pamplona, Spain. [2]Centro de Investigación Biomédica en Red-Fisiopatología de la Obesidad y Nutrición (CIBEROBN), Instituto de Salud Carlos III, Pamplona, Spain. [3]Obesity and Adipobiology Group, Instituto de Investigación Sanitaria de Navarra (IdiSNA), Pamplona, Spain. [4]Institute for Nutrition & Health, University of Navarra, Pamplona, Spain. [5]Department of Endocrinology & Nutrition, Clínica Universidad de Navarra, Pamplona, Spain

[Received June 21, 2026; Revised September 8, 2026; Accepted September 12, 2026]

ABSTRACT: Growth differentiation factor 15 (GDF15) is a regulator of body weight and systemic homeostasis. However, the mechanisms underlying its effects remain unclear. This study aimed to determine whether diet, age, and sex influence GDF15's metabolic effects. Male and female mice aged 8 or 64 weeks were fed a normal diet (ND) or high-fat diet (HFD) for 20 weeks and were treated subcutaneously with recombinant GDF15 or vehicle for 3 weeks. Body weight and food intake were monitored. Epididymal white adipose tissue (eWAT), subcutaneous WAT (scWAT), brown adipose tissue (BAT), liver, and gastrocnemius muscle were analyzed by histology and gene expression. GDF15 reduced body weight, with greater effects in HFD-fed and aged mice. Reduced food intake was mainly observed in young HFD-fed mice. GDF15 improved glycemic control and exerted tissue-, diet-, and age-dependent effects. The liver showed greater transcriptional changes, especially in aged mice, although GDF15 also induced tissue-specific changes in BAT, gastrocnemius muscle, and eWAT. *Gdf15* expression was more strongly induced by HFD in BAT and by aging in eWAT. These findings reveal that GDF15 exerts robust metabolic effects on body weight and glucose homeostasis, with age-dependent effects on food intake. GDF15 induced tissue-specific responses influenced by diet and age that may contribute to its systemic effects. These findings suggest that additional mechanisms beyond reduced food intake may contribute to the greater weight loss observed in aged mice. Together, our findings highlight age as a key determinant of the systemic response to GDF15.

Keywords: GDF15 treatment, obesity, aging, weight loss, metabolic homeostasis

INTRODUCTION

The prevalence of obesity has increased dramatically over recent decades, representing a major global health challenge closely linked to metabolic and cardiovascular disorders. This trend underscores the urgent need to identify novel therapeutic strategies [1, 2]. Growth differentiation factor 15 (GDF15) is a member of the transforming growth factor beta (TGF-β) superfamily involved in metabolic regulation [3-5]. Notably, GDF15 is broadly expressed across multiple tissues [3], and its circulating levels increase in response to cellular stress and tissue injury, supporting its role as a stress-responsive cytokine [6, 7]. In fact, GDF15 has recently been highlighted as one of the best markers of systemic stress [8]. GDF15 signals through the glial cell-derived neurotrophic factor family receptor alpha-like (GFRAL)/ tyrosine kinase co-receptor RET complex. GFRAL expression has been reported to be limited to the central nervous system, particularly the brainstem [9-12],

***Correspondence should be addressed to:** Dr. Javier Gómez-Ambrosi, Metabolic Research Laboratory, Clínica Universidad de Navarra, Pamplona, Spain. Email: jagomez@unav.es

Copyright: © 2026 Salmón-Gómez L. et al. This is an open-access article distributed under the terms of the Creative Commons Attribution License, which permits unrestricted use, distribution, and reproduction in any medium, provided the original author and source are credited.

although very low but detectable levels have also been detected in some peripheral tissues [13, 14]. Nevertheless, accumulating evidence indicates that GDF15 exerts peripheral actions, suggesting that additional receptors may contribute to mediating its effects [15].

Since the identification of GDF15 as a metabolic regulator, numerous studies have investigated its physiological and therapeutic effects. GDF15 levels are elevated in obesity in both preclinical animal models and human studies [16-19] as well as during aging [18, 20] and in age-related disorders [21, 22]. Overexpression or pharmacological administration of GDF15 induces weight loss [23], preferentially reducing fat mass rather than lean mass, with more pronounced effects in mice fed a HFD [24]. Consistently, loss of GDF15 blunts these effects and promotes increased body weight gain [12, 23, 25]. However, the mechanisms underlying these effects remain controversial. While several studies have reported that GDF15 reduces body weight primarily through anorexigenic effects without significant effects on energy expenditure [10, 26, 27], others have shown that GDF15 not only decreases food intake but also increases energy expenditure [24, 28, 29] or increases energy expenditure alone [30]. GDF15 has been shown to promote energy expenditure by upregulating thermogenesis in adipose tissue [24] as well as by sustaining fatty acid oxidation and calcium futile cycling in skeletal muscle [28]. The discrepancies regarding the effects of GDF15 may depend on the experimental model [29] and some studies suggest sex-specific responses to GDF15 treatment [23, 31]. Beyond its effects on body weight, GDF15 overexpression improves glucose tolerance [24, 26, 28, 32], enhances insulin sensitivity [28, 32], reduces inflammation [24], partly through a reduction in pro-inflammatory cytokines and macrophage infiltration [22, 33], and may increase lifespan [32].

Therefore, although GDF15 has been proposed as a potential therapeutic target for weight loss, its effects appear to be context-dependent. We herein hypothesized that GDF15 effects might be influenced by age and diet. Therefore, the aim of this study was to investigate the effects of GDF15 treatment across different contexts by integrating multiple variables, including diet and age, to determine whether these factors influence the metabolic outcomes of GDF15 treatment. Potential sex-related differences were explored as a secondary analysis.

MATERIALS AND METHODS

Experimental model

Male and female C57BL/6J mice were purchased from The Jackson Laboratory (Bar Harbor, ME, USA) at 8 or 64 weeks of age and maintained under a controlled temperature of 22 ± 2 ºC, with relative humidity (50 ± 10%) and a 12 h dark and 12 h light cycle. Upon arrival, mice were fed *ad libitum* either a normal diet (ND) (2014S Teklad Global 14% Protein Rodent Maintenance Diet, Harlan, Barcelona, Spain) or a 60% HFD (Diet #F3282, Bio-Serve, Frenchtown, NJ, USA) for 20 weeks. The ND and HFD were commercially available diets, not matched for protein or micronutrient composition, while ensuring that all nutritional requirements were met. At the end of the dietary intervention, mice were approximately 28 or 84 weeks of age and were subcutaneously treated with either vehicle (physiological saline) or recombinant human GDF15 (0.2 µg per g body weight) at the start of the light cycle for 3 weeks (3 days per week). Recombinant human GDF15 was used due to the conserved nature of the GDF15-GFRAL signaling axis and its demonstrated biological activity in mice, consistent with the expected cross-species activity [10, 11]. The experimental model is represented in Figure 1A, which includes the number of animals per group and sex distribution. Body weight and food intake were registered once weekly before treatment and then on each treatment day. Food intake was measured per cage and expressed as the average daily food intake per mouse. All experimental procedures conformed to the European Guidelines for the Care and Use of Laboratory Animals (directive 2010/63/EU). The study was approved by the Ethical Committee for Animal Experimentation of the University of Navarra (021/20).

Blood and tissue collection

At the end of the study, mice were sacrificed by CO_2 inhalation under fasting conditions approximately 24 h after the last treatment administration. Blood was collected and serum samples were obtained after centrifugation at 700 *g* for 15 min at 4 °C, and stored at −80 °C. The entire epididymal white adipose tissue (eWAT), subcutaneous WAT (scWAT), perirenal WAT (prWAT) and brown adipose tissue (BAT), as well as the liver and both gastrocnemius muscles, were carefully excised, weighed, and divided for either paraformaldehyde fixation or flash freezing and storage at -80 ºC. Total adiposity was considered as the sum of eWAT, scWAT, and prWAT.

Intraperitoneal glucose tolerance tests

Intraperitoneal glucose tolerance tests (IPGTTs) were conducted in mice the day before sacrifice. IPGTTs were performed after overnight fasting (12 h). Blood glucose was assessed automatically by a glucometer (Ascensia Elite, Bayer, Barcelona, Spain) by tail bleeds at baseline (fasting blood glucose) and at 15, 30, 60 and 120 min after

the administration of 50% D-glucose solution (2 g/kg of BW). The area under the curve (AUC) was calculated according to the trapezoidal method as previously reported [34].

Measurements of circulating metabolites and hormones

Circulating GDF15 (MGD150, R&D Systems, Minneapolis, MN, USA), insulin (90080; Crystal Chem, Elk Grove Village, IL, USA), serum amyloid A (SAA) (MSAA00; R&D), osteopontin (OPN) (MOST00; R&D Systems), adiponectin (RD293023100R; BioVendor) leptin (90030; Crystal Chem,) and tumor necrosis factor alpha (TNF-α) (MHSTA50; R&D Systems,) were quantified using commercial kits according to the manufacturers' instructions. The intra- and inter-assay coefficients of variation were <8% and <10%, respectively, across all ELISAs performed. Serum and liver triglycerides (TG) levels (Wako Chemicals, GmbH, Neuss, Germany) and total cholesterol (Infinity, Thermo Electron Corporation, Melbourne, Australia) were measured by enzymatic photometric tests. The homeostatic model assessment (HOMA-IR) and the quantitative insulin sensitivity check index (QUICKI) were calculated to estimate insulin resistance or insulin sensitivity, respectively.

Histological analysis

Adipocyte size was assessed by measuring the cross-sectional area (CSA) of adipocytes in eWAT samples. Tissue samples from each mouse were formalin-fixed and paraffin-embedded (4 µm). Sections were stained with hematoxylin-eosin for morphometric analysis. Images from 4 sections per animal were randomly acquired with a ×20 objective and the adipocyte CSA was quantified using AxioVision Release 4.6.3 software (Zeiss, Göttingen, Germany), as previously described [34].

Lipid droplet content in BAT was quantified by analyzing lipid droplet areas in haematoxylin-eosin-stained tissue sections. Tissue samples from BAT were formalin-fixed and paraffin-embedded. Sections (4 µm) were stained with hematoxylin–eosin for morphometric analysis. Images of 6 sections per animal were randomly captured at ×20 objective, and lipid droplet area was quantified using ImageJ software, version 1.54g (https://imagej.nih.gov/ij) (National Institutes of Health, Bethesda, USA). Lipid droplets were identified as optically lipid droplet areas, and a consistent thresholding approach was applied to segment them.

For fibrosis quantification, sections of formalin-fixed paraffin-embedded liver tissue (6 µm) were dewaxed with xylene, rehydrated through graded ethanol solutions and stained with 1% Sirius red (Sigma, St. Louis, MO, USA) to detect collagen fibers. Images were acquired from 3 randomly selected fields per section per animal at ×20 objective magnification. Fibrotic area was quantified as the proportion of Sirius-Red-positive staining relative to the total area using ImageJ software, version 1.54g (National Institutes of Health), as previously described [35]. Investigators performing histological quantification of adipocyte size, BAT lipid droplet area, and liver fibrosis were blinded to the experimental groups.

RNA isolation and quantitative RT-PCR analysis

Total RNA was isolated from eWAT, scWAT, BAT, and liver using the QIAzol® Reagent (Invitrogen, Barcelona, Spain), and from gastrocnemius using RTL buffer + β-mercaptoethanol, followed by purification with the RNeasy Lipid Tissue kit (Qiagen, Hilden, Germany) for WAT and BAT, the RNeasy Tissue Mini Kit (Qiagen) for the liver, and the RNeasy Fibrous Tissue Mini Kit (Qiagen) for gastrocnemius. RNA concentrations were determined by measuring absorbance at 260 nm, and samples were treated with DNase I (RNase-free DNase Set, Qiagen). First-strand cDNA synthesis was performed by reverse transcription of 3 µg of total RNA, as previously described [36]. The cDNA was amplified using the TaqMan® Universal PCR Master Mix (Applied Biosystems, Foster City, CA, USA) and the transcript levels of the target genes were quantified by real-time PCR (7300 Real-Time PCR System; Applied Biosystems). The thermal cycling conditions were as follows: 95 °C for 10 min, followed by 45 cycles of 15 s at 95 °C and 1 min at 59 °C. Gene expression levels were normalized to *18S* rRNA (Applied Biosystems) and relative expression was calculated using the $2^{-\Delta\Delta Ct}$ formula [37]. Gene-specific primers and probes were designed using Primer Express 2.0 software (Applied Biosystems) and are listed in Supplementary Table 1.

Statistical analysis

Data were summarized using the mean ± standard error of the mean (SEM). Normality of the data distribution was assessed using the Shapiro-Wilk test. Primary analyses focused on the main phenotypic and metabolic outcomes using pooled male and female data to maximize statistical power, whereas gene expression analyses were considered exploratory and were performed on a predefined panel of biologically relevant genes. Differences between groups were tested by three-way analysis of variance (ANOVA). When significant treatment x age, treatment x diet, or treatment x age x diet interactions were detected, two-way ANOVA followed by Student's *t*-tests when necessary were performed.

Significant diet x age interactions identified in the three-way ANOVA were also explored using Student's *t*-test. For datasets not following a Gaussian distribution, logarithmic transformation was applied, and statistical analysis was performed using ANOVA on the transformed values. An exploratory four-way ANOVA including sex as an additional factor was also performed (Supplementary Table 2). This analysis was not used for primary inference, as the inclusion of sex as fourth factor increased model complexity and reduced the sample size within each subgroup, limiting the statistical power to detect higher-order interactions. Correlation analyses were performed using Spearman's rank correlation coefficient, given the non-normal distribution of some variables analyzed. All statistical analyses were performed using the GraphPad Prism software (v.10.1.1) as well as the SPSS software, version 25.0 (SPSS Inc., Chicago, IL, USA) Statistical significance was considered at $P \leq 0.05$.

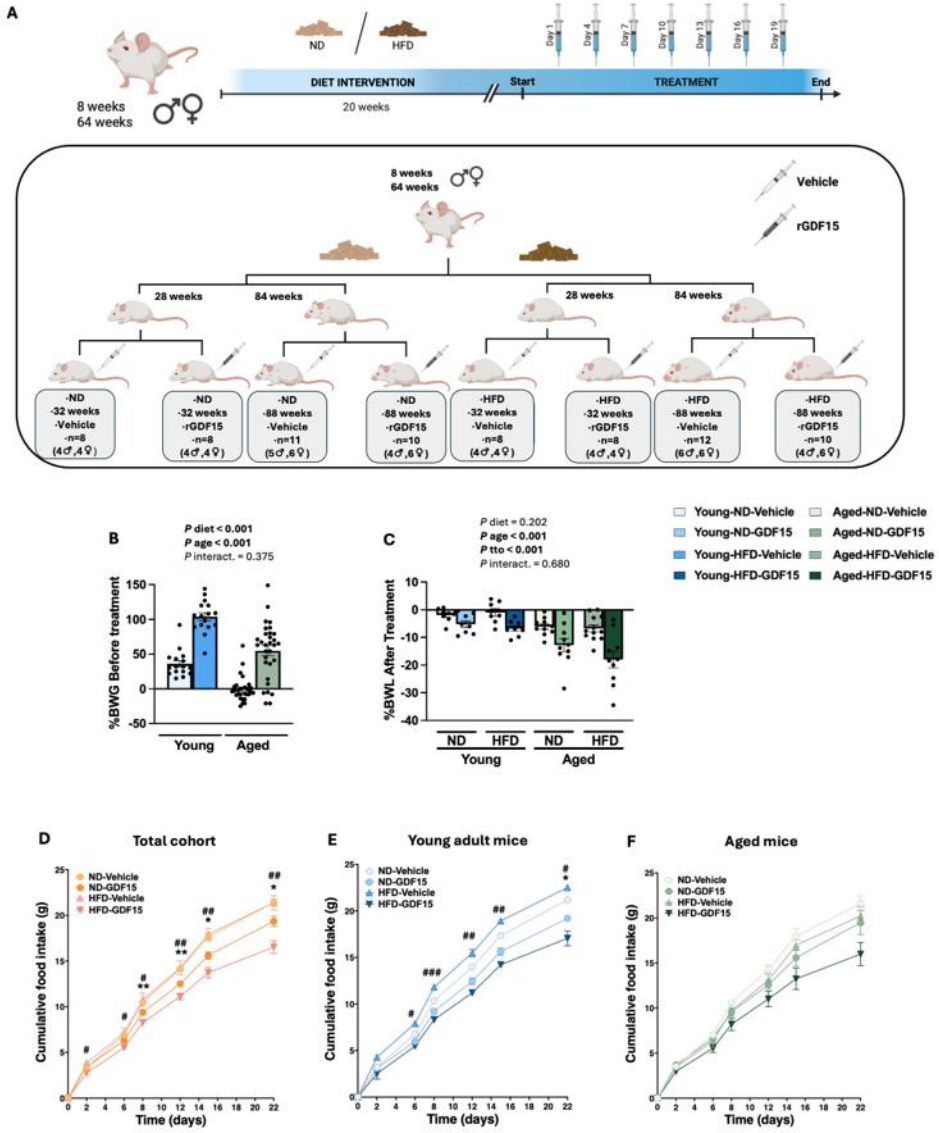


Figure 1. Experimental design and effects of GDF15 on body weight and food intake. (A) Experimental design. **(B)** Percentage of body weight gain (%BWG) before GDF15 treatment. **(C)** Percentage of body weight loss (%BWL) after GDF15 treatment. **(D)** Cumulative food intake during GDF15 treatment in all groups, as well as in **(E)** young and **(F)** aged mice. Data are presented as the mean ± SEM. Exact sample sizes for each analysis are provided in Supplementary Table 3. Differences between groups were tested by two- or three-way ANOVA and Student's *t*-tests. Only significant partial interactions between factors were represented. $*P < 0.05$, $**P < 0.01$; $^{\#}P < 0.05$, $^{\#\#}P < 0.01$, $^{\#\#\#}P < 0.001$. * indicates comparisons between ND-vehicle and ND-GDF15 groups, whereas # indicates comparisons between HFD-vehicle and HFD-GDF15 groups.

RESULTS

GDF15 administration is more effective in reducing body weight in aged mice than in young mice

Before treatment, HFD-fed mice exhibited a greater body weight gain than those fed a ND in both young and aged groups (Fig. 1B). Moreover, young mice gained more body weight than aged mice (Fig. 1B). Following GDF15 treatment, body weight was significantly reduced across all experimental groups (Fig. 1C). Interestingly, GDF15 administration appeared to be more effective in reducing body weight in HFD-fed and aged mice (Fig. 1C). In line with these results, GDF15 treatment induced a greater reduction in food intake in HFD-fed mice compared with ND-fed mice (Fig. 1D). However, when age groups were analyzed separately, the effect of GDF15 on food intake differed between young and aged mice (Fig. 1E-F). In young mice, GDF15 treatment significantly reduced food intake in HFD-fed mice from day 6 of treatment, whereas in ND-fed mice, the effect was only significant at the end of the treatment (Fig. 1E). In contrast, GDF15 treatment did not significantly reduce food intake in aged mice (Fig. 1F). Therefore, these findings suggest that GDF15 may act through additional mechanisms beyond the regulation of food intake to account for the greater weight loss observed in aged mice compared with young mice, which was not accompanied by a reduction in food intake.

Regarding body composition, HFD feeding increased the weight of measured tissues, with the exception of the soleus muscle (Supplementary Fig. 1A-H). Although GDF15 treatment did not significantly reduce WAT depots (Supplementary Fig. 1A-B), it showed a trend toward reducing total AT (P=0.076) (Supplementary Fig. 1C). Notably, GDF15 significantly reduced the weights of BAT (Supplementary Fig. 1D), heart, and spleen (Supplementary Fig. 1E), and showed a tendency to reduce liver mass (P=0.078) (Supplementary Fig. 1F) without affecting muscle mass (Supplementary Fig. 1G-H) or kidney weight (Supplementary Fig. 1E).

GDF15 improves systemic metabolic homeostasis independently of diet and age

Given the significant reduction in body weight accompanied by modest changes in tissue mass, we next evaluated whether GDF15 administration induced systemic metabolic adaptations by analyzing several circulating metabolic parameters. Fasting glucose levels were increased by HFD-feeding, with a tendency toward lower glycemia following GDF15 treatment in HFD-fed mice (Fig. 2A). Consistently, although no significant differences were observed in the IPGTT curves (Supplementary Fig. 2A-B), glucose AUC was significantly increased in HFD-fed mice and reduced following GDF15 treatment (Fig. 2B), suggesting improved glucose tolerance after treatment. Similarly, circulating insulin levels were significantly increased by HFD and reduced following GDF15 treatment (Fig. 2C). Consistent with this, mice treated with GDF15 exhibited improved indices of insulin sensitivity, as reflected by increased QUICKI values (Fig. 2D) and reduced HOMA-IR (Fig. 2E). Regarding lipid metabolism, HFD increased circulating TG and cholesterol levels (Fig. 2F-G). GDF15 significantly reduced TG concentrations (Fig. 2F), while total cholesterol was not significantly altered, although a trend toward reduction was observed (P=0.078) (Fig. 2G). Additionally, circulating adiponectin concentrations remained unchanged (Fig. 2H), while leptin levels were increased by HFD and reduced by treatment (Fig. 2I). Consequently, the adiponectin/leptin ratio was significantly increased following GDF15 treatment (Fig. 2J). GDF15 treatment did not significantly alter circulating levels of the inflammatory markers OPN, SAA, or TNF-α (Supplementary Fig. 2C-E), which were increased by HFD and aging. Additionally, whereas circulating GDF15 concentrations were also increased by diet and age, exogenous GDF15 administration did not modulate circulating GDF15 levels, consistent with its short half-life in circulation (approximately 3 h) [38] (Supplementary Fig. 2F).

Adipose tissue shows the strongest upregulation of *Gdf15* expression in response to HFD feeding and aging

To assess the tissue-specific changes in *Gdf15* mRNA expression induced by HFD and aging, mRNA levels across metabolically relevant tissues were quantified, including liver, eWAT, scWAT, BAT, and gastrocnemius muscle. HFD significantly increased *Gdf15* expression in all tissues analyzed (Fig. 3A-E). Aging also significantly increased *Gdf15* expression across all tissues, except in the liver (P=0.098) (Fig. 3A-E). Interestingly, in young mice, pronounced HFD-induced changes in *Gdf15* expression were observed in BAT and eWAT (28.1- and 12.4-fold increases, respectively). Furthermore, aging induced the greatest increase in *Gdf15* expression in eWAT (9.9-fold increase). GDF15 treatment significantly reduced *Gdf15* mRNA expression in BAT of young mice and showed a trend toward reduction in the liver of young ND-fed and aged mice (P=0.056), as well as in gastrocnemius muscle, independently of diet and age (P=0.058).

To further evaluate the relationship between tissue-specific *Gdf15* expression and circulating GDF15 levels, correlation analysis was performed (Fig. 3F). In control ND-fed mice, circulating GDF15 levels were positively

associated with *Gdf15* expression in eWAT and BAT, whereas under HFD conditions, this association was primarily maintained with eWAT. Following GDF15 administration, significant positive correlations were observed in eWAT, BAT, and gastrocnemius muscle under both ND and HFD conditions.

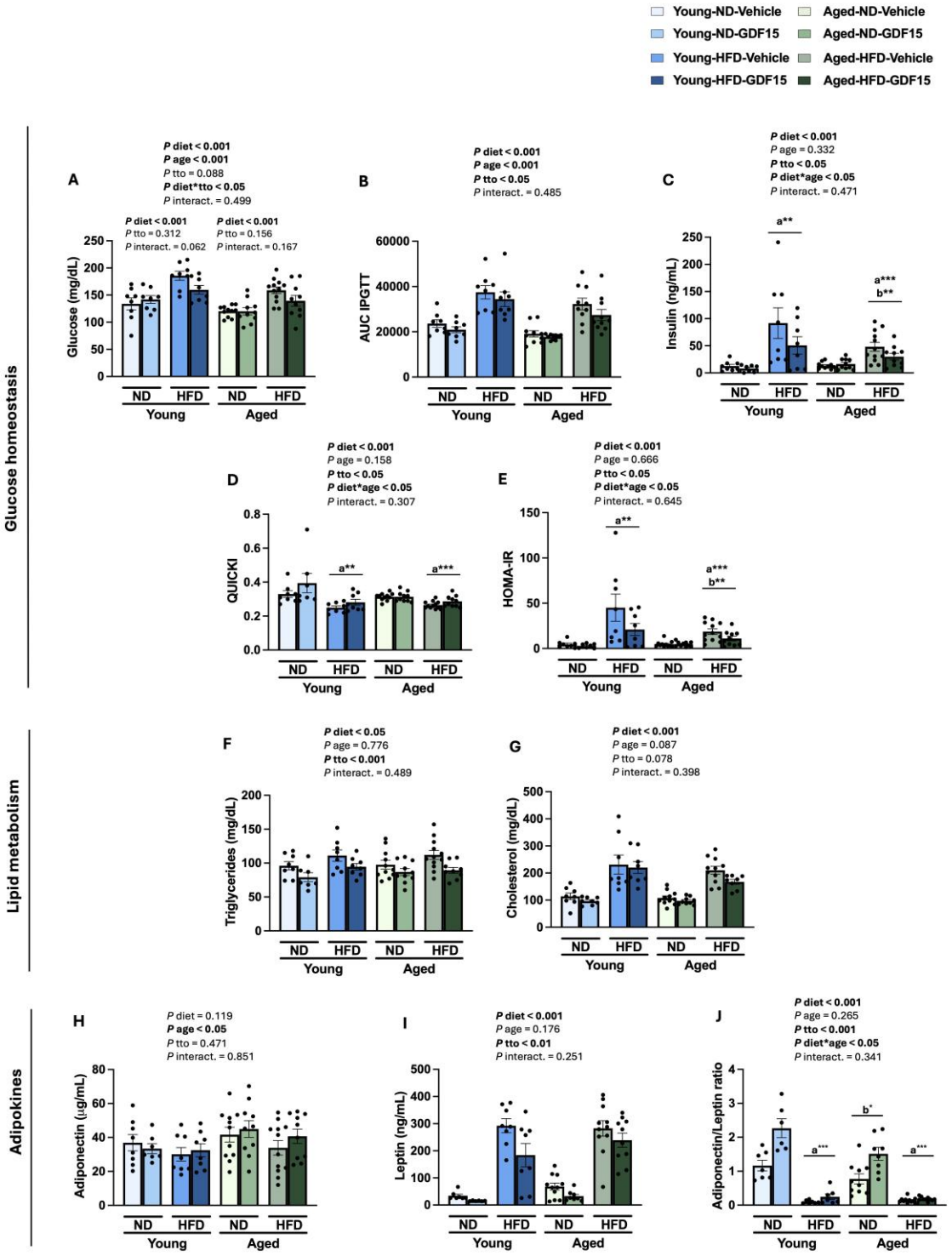


Figure 2. Glucose homeostasis and circulating metabolic parameters. Circulating concentrations of serum variables. **(A-E):** Glucose homeostasis markers: circulating levels of **(A)** glucose, **(B)** AUC of intraperitoneal glucose tolerance test (IPGTT) and **(C)** insulin and calculated indices **(D)** QUICKI and **(E)** HOMA-IR. **(F-G)** Lipid metabolism markers: circulating levels of **(F)** triglycerides and **(G)**

total cholesterol. Adipokines: circulating concentrations of **(H)** adiponectin and **(I)** leptin and **(J)** adiponectin/leptin ratio. Data are presented as the mean ± SEM. Exact sample sizes for each analysis are provided in Supplementary Table 3. Differences between groups were tested by three- or two-way ANOVA followed by Student's *t*-tests when necessary. *P* values displayed at the top of each graph correspond to three-way ANOVA results, whereas the additional *P* values shown below correspond to subsequent two-way ANOVA analyses performed when significant interactions were detected in the three-way ANOVA. Only significant partial interactions between factors were represented. The letters indicate Student's *t*-test comparisons. a denotes HFD vs. ND comparisons within the same age group; b denotes young vs. old comparisons within the same type of diet. **P* < 0.05, ***P* < 0.01, ****P* < 0.001.

To evaluate peripheral *Gfral* expression, two independent assays targeting different regions of the *Gfral* transcript were used. While one assay did not detect *Gfral* expression in peripheral tissues, the other consistently detected very low *Gfral* expression in liver and gastrocnemius, with no significant effects of diet or aging (Supplementary Fig. 3A-B). The detection of low expression with one assay, together with the absence of detectable expression with the second assay, raises the possibility that *Gfral* may be expressed in some peripheral tissues at very low levels, close to the detection limit of qPCR. However, peripheral *Gfral* expression remains uncertain and would require independent validation. In the assay detecting low *Gfral* expression, *Gfral* expression in gastrocnemius was increased following GDF15 administration in young mice, whereas it was reduced in aged ND-fed mice (Supplementary Fig. 3B).

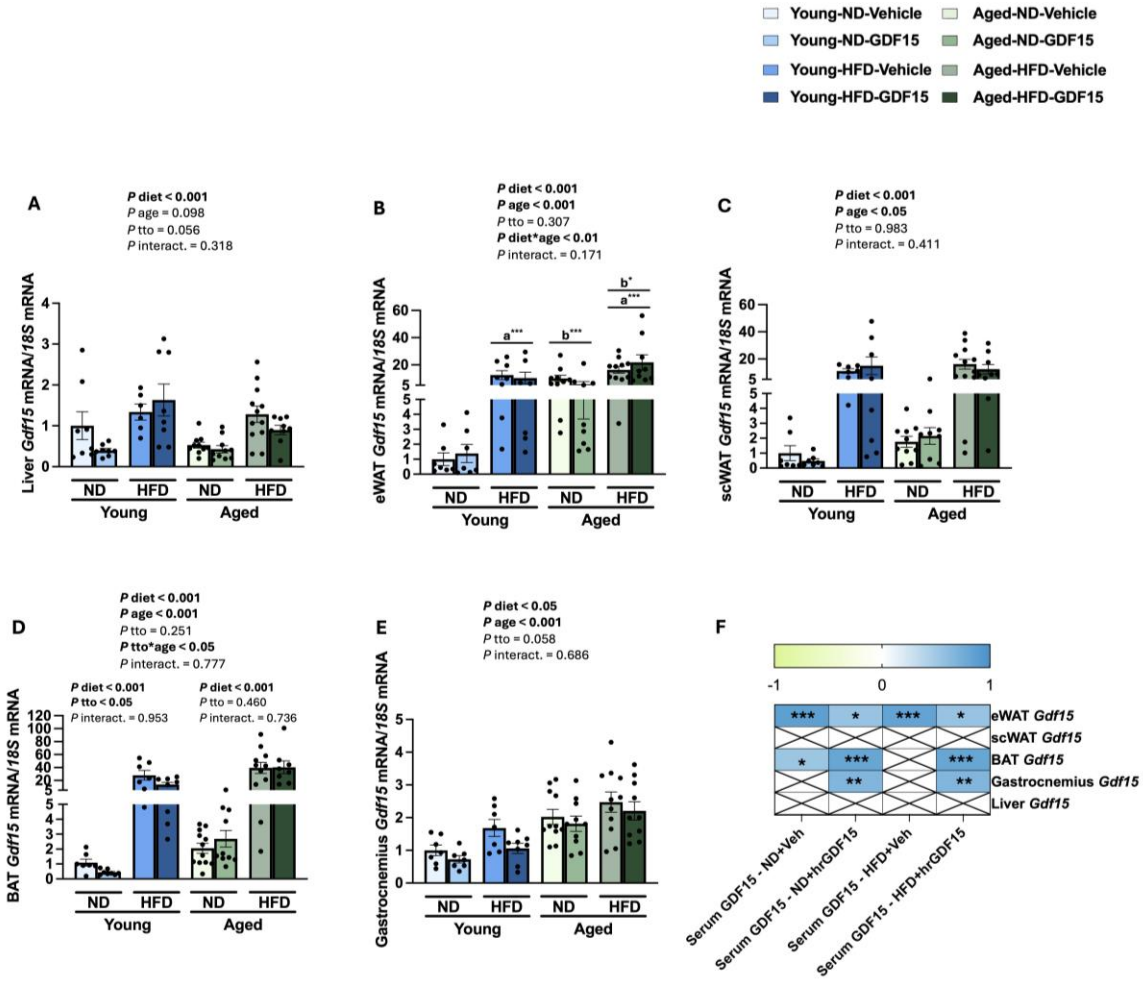


Figure 3. Tissue-specific *Gdf15* mRNA expression and correlations with circulating GDF15 concentrations. Relative mRNA expression of *Gdf15* in **(A)** liver, **(B)** epididymal white adipose tissue (eWAT), **(C)** subcutaneous white adipose tissue (scWAT), **(D)** brown adipose tissue (BAT) and **(E)** gastrocnemius, as well as **(F)** their correlations with serum GDF15 concentrations. Data are presented as the mean ± SEM. Exact sample sizes for each analysis are provided in Supplementary Table 3. Differences between groups were tested by three- or two-way ANOVA followed by Student *t*-tests when necessary. *P* values displayed at the top of each graph correspond to three-way ANOVA results, whereas the additional *P* values shown below correspond to subsequent two-way ANOVA

analyses performed when significant interactions were detected in the three-way ANOVA. Only significant partial interactions between factors were represented. Correlation analyses were performed using Spearman's rank correlation coefficient. The letters indicate Student's *t*-test comparisons. a denotes HFD vs. ND comparisons within the same age group; b denotes young vs. old comparisons within the same type of diet. **P* < 0.05, ***P* < 0.01, ****P* < 0.001.

GDF15 has limited and context-dependent effects on adipose tissue

Given the robust induction of *Gdf15* in adipose tissue depots, cellular and molecular adaptations to HFD and aging, as well as the effects of GDF15, were examined in eWAT. HFD feeding induced adipocyte hypertrophy, evidenced by increased adipocyte size (Fig. 4A-B). GDF15 treatment tended to decrease adipocyte size in ND-fed mice and to increase it in HFD-fed mice, although these differences did not reach statistical significance (Fig. 4B).

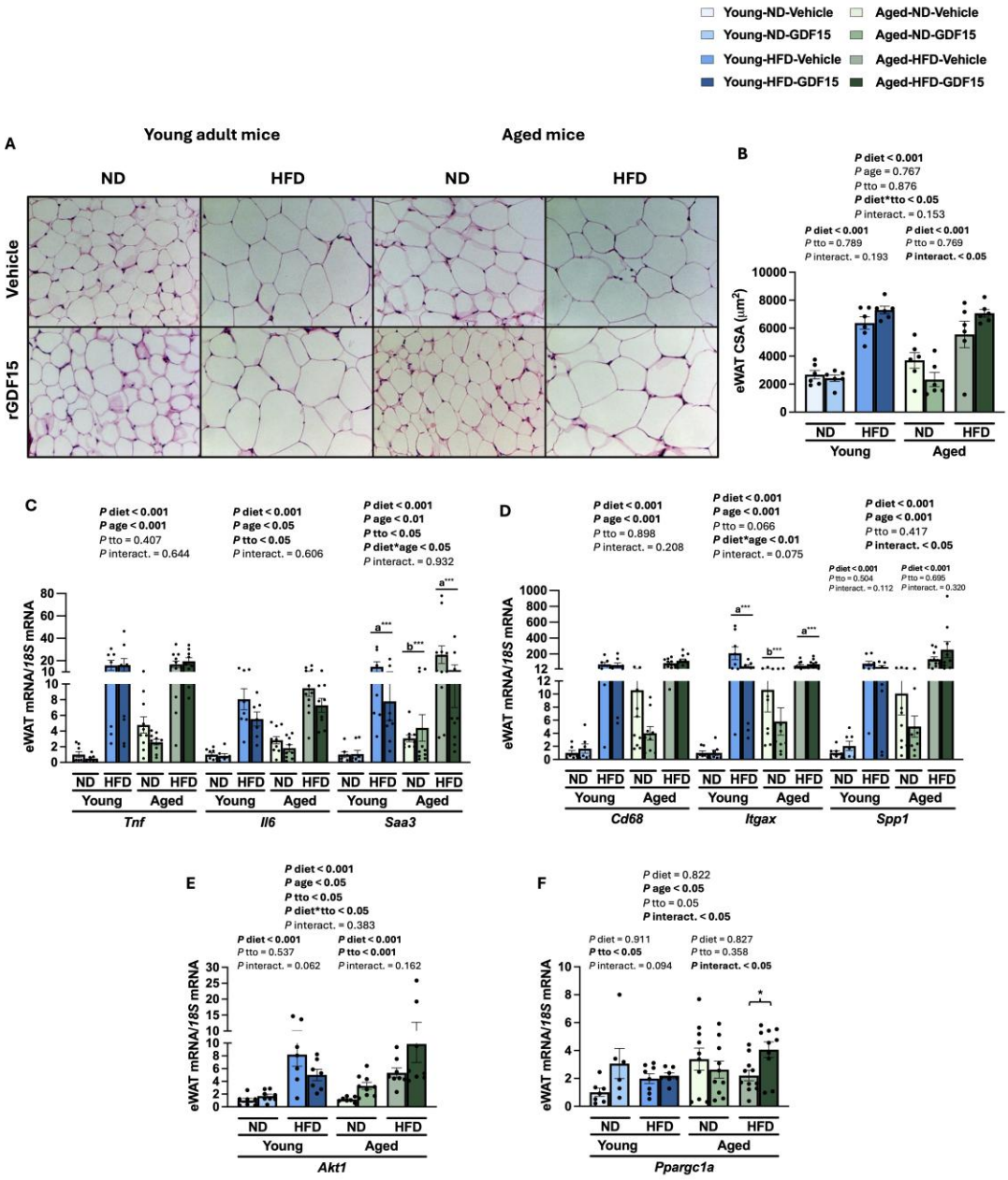


Figure 4. Epididymal adipose tissue morphology and gene expression. (A) Hematoxylin and eosin staining of epididymal adipose tissue (eWAT) (magnification ×200). Quantification of **(B)** adipocyte size. Relative mRNA expression of selected genes in eWAT: **(C)** *Tnf, Il6* and *Saa3*; **(D)** *Cd68, Itgax,* and *Spp1*; **(E)** *Akt1*; **(F)** *Ppargc1a.* Data are presented as the mean ± SEM. Exact sample sizes for each analysis are provided in Supplementary Table 3. Differences between groups were tested by three- or two-way ANOVA followed by Student's *t*-tests when necessary. *P* values displayed at the top of each graph correspond to three-way ANOVA results, whereas the additional *P* values shown below correspond to subsequent two-way ANOVA analyses performed when significant interactions were detected in the three-way ANOVA. Only significant partial interactions between factors were represented. The letters and asterisks indicate Student's *t*-test comparisons. a denotes HFD vs. ND comparisons within the same age group; b denotes young vs. old comparisons within the same type of diet. $*P < 0.05$, $***P < 0.001$.

In parallel, HFD and aging elicited a robust inflammatory response in eWAT, characterized by increased mRNA expression of pro-inflammatory markers (*Tnf*, *Il6* and *Saa3*) (Fig. 4C), macrophage markers (*Cd68*, *Itgax*/*Cd11c* and *Spp1*) (Fig. 4D), and interleukin-related genes (*Il1a*, *Il1b* and *Il1ra*) (Supplementary Fig. 4A). GDF15 treatment was associated with limited reductions in the expression of inflammatory genes, including reduced *Il6* expression independently of diet and age (Fig. 4C) and *Saa3* expression in HFD-fed mice (Fig. 4C). These changes were accompanied by alterations in adipokine expression, with HFD upregulating *Adipoq* and *Lep* expression (Supplementary Fig. 4B). Notably, GDF15 administration further increased *Adipoq* expression in young HFD-fed mice. Similarly, HFD also increased *Adipoq* and *Lep* expression in scWAT, although GDF15 treatment did not significantly modify their expression (Supplementary Fig. 5A).

We then examined metabolic adaptations in eWAT. HFD increased *Atgl* expression, a regulator of lipolysis, while decreasing *Acaca* expression (Supplementary Fig. 4C), a key enzyme involved in lipogenesis, indicating differential regulation of genes involved in lipid metabolism. *Akt1*, an insulin-signaling gene, was also upregulated by HFD (Fig. 4E), with GDF15 treatment further increasing *Akt1* expression in aged mice independently of diet. In contrast, the expression of key regulators of adipocyte lipid metabolism, including *Ppara* and *Pparg*, was generally unaffected by diet, age, or treatment, although HFD increased *Pparg* expression (Supplementary Fig. 4D).

Given the reported involvement of GDF15 in mitochondrial function, we next assessed the mRNA expression of *Ppargc1a*, a master regulator of mitochondrial biogenesis, together with genes encoding subunits of mitochondrial electron transport chain complexes (*Ndufa6*, *Sdhc*, *Uqcrb*, *Cox4i1* and *Atp5b*). HFD feeding had no effect on *Ppargc1a* expression (Fig. 4F) but upregulated the expression of mitochondrial genes independently of age (Supplementary Fig. 4E). GDF15 selectively increased *Ppargc1a* expression in young mice and in aged HFD-fed mice without affecting mitochondrial gene expression (Fig. 4F, Supplementary Fig. 4E). In scWAT, HFD increased *Ppargc1a* expression, and GDF15 treatment also upregulated its expression in young ND-fed mice (Supplementary Fig. 5B). Similarly, HFD increased mitochondrial gene expression, whereas these genes were not significantly altered by GDF15 treatment (Supplementary Fig. 5C).

Additionally, HFD induced the expression of extracellular matrix (ECM) remodeling (*Col6a3*, *Mmp14*, *Tgfb1, Lox* and *Thbs1*) and angiogenic genes (*Kdr*, *Fgf2* and *Angpt2),* consistent with tissue remodeling (Supplementary Fig. 6A-C). GDF15 treatment had modest effects, reducing *Col6a3*, *Thbs1* and *Fgf2* expression in aged mice.

Altogether, these findings indicate that HFD and aging induced broad morphological and transcriptional changes in eWAT, including alterations in inflammatory and metabolism-related gene expression, with GDF15 selectively modulating specific aspects of this response.

GDF15 treatment selectively modulates thermogenic and inflammatory gene expression in BAT

To further investigate potential mechanisms underlying the observed differences in body weight, we next examined BAT to investigate whether GDF15 was associated with changes in the expression of thermogenesis-related genes.

Histological analysis demonstrated increased lipid accumulation in BAT in response to HFD, as reflected by an increased percentage of lipid droplet area (Fig. 5A-B), indicative of BAT whitening. Notably, GDF15 treatment reduced lipid accumulation across all experimental groups (Fig. 5B).

Analysis of mitochondrial and thermogenic regulators revealed that HFD feeding increased *Ucp1* and *Ppargc1a* expression (Fig. 5C-D), without altering the expression of *Prdm16, Cidea* or *Cpt1b* (Fig. 5E), genes involved in brown adipocyte reprogramming, lipid droplet regulation and fatty acid oxidation, respectively. Notably, GDF15 treatment increased *Ppargc1a* expression across all experimental groups (Fig. 5D), and selectively increased *Prdm16* expression in young mice (Fig. 5E). HFD also increased the expression of *Sdhc*, *Cox4i1* and *Atp5b,* whereas GDF15 administration did not modify their expression (Supplementary Fig. 7A).

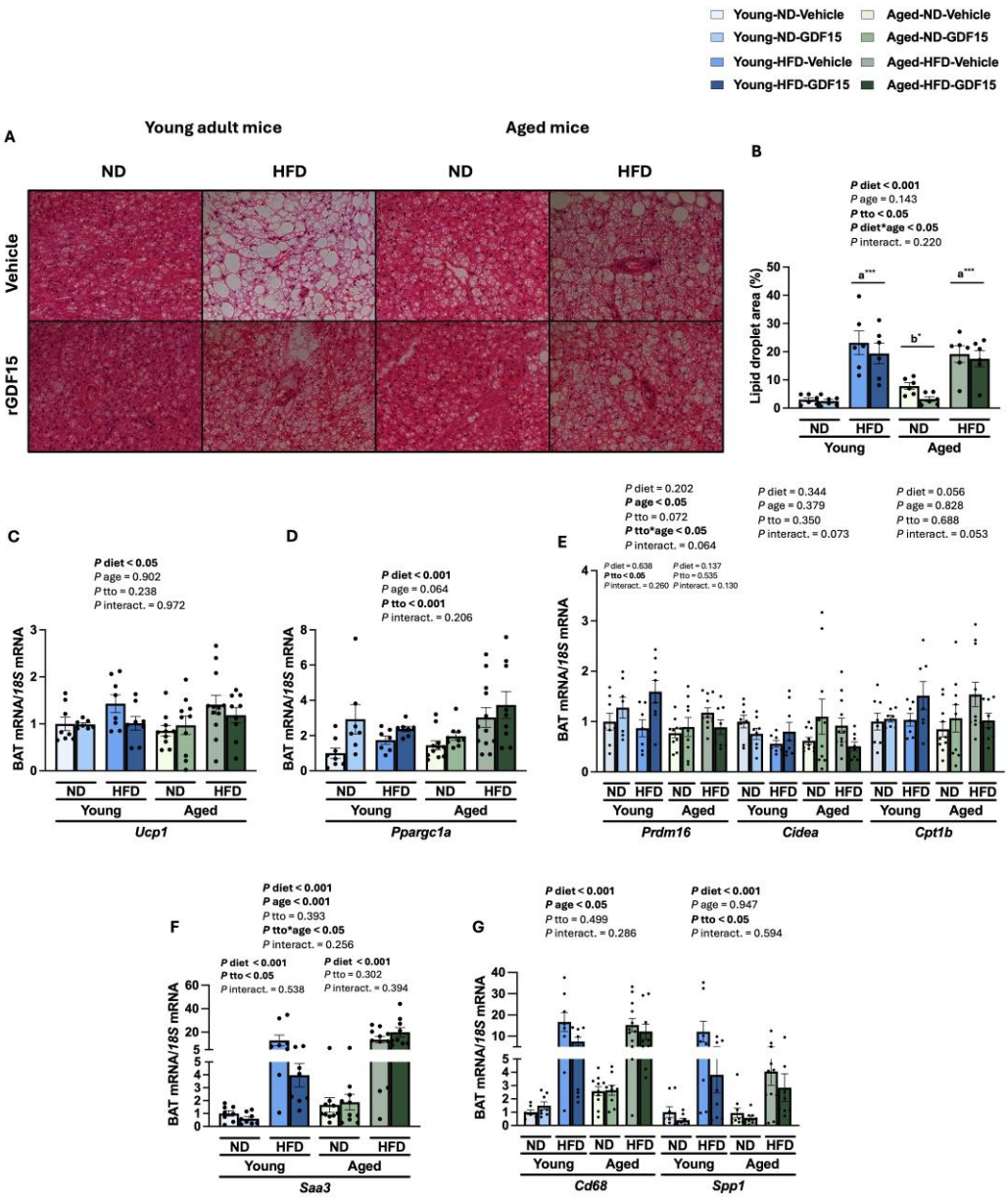


Figure 5. Brown adipose tissue morphology and gene expression. (A) Hematoxylin and eosin staining of BAT (magnification ×200) and **(B)** lipid droplet area (%). Relative mRNA expression of selected genes in brown adipose tissue (BAT): **(C)** *Ucp1*; **(D)** *Ppargc1a;* **(E)** *Prdm16, Cidea* and *Cpt1b*; **(F)** *Saa3* **(G)** *Cd68* and *Spp1*. Data are presented as the mean ± SEM. Exact sample sizes for each analysis are provided in Supplementary Table 3. Differences between groups were tested by three- or two-way ANOVA followed by Student's *t*-tests when necessary. *P* values displayed at the top of each graph correspond to three-way ANOVA results, whereas the additional *P* values shown below correspond to subsequent two-way ANOVA analyses performed when significant interactions were detected in the three-way ANOVA. Only significant partial interactions between factors were represented. The letters indicate Student's *t*-test comparisons. a denotes HFD vs. ND comparisons within the same age group; b denotes young vs. old comparisons within the same type of diet. **P* < 0.05, ****P* < 0.001.

As expected, HFD feeding significantly increased the mRNA expression of inflammatory markers (*Saa3*, *Cd68* and *Spp1*) in both young and aged mice (Fig. 5F-G). GDF15 treatment significantly decreased *Saa3* expression in young mice as well as *Spp1* independently of age (Fig. 5G-H), indicating a partial modulation of the inflammatory gene expression profile.

Moreover, HFD induced the expression of genes related to ECM remodeling in BAT, as indicated by increased *Mmp14* (Supplementary Fig. 7B) and *Col6a3*

(Supplementary Fig. 7C) expression. GDF15 treatment showed a trend towards reduced *Mmp14* expression, mostly in HFD-fed mice ($P = 0.052$), with no significant effect on *Col6a3*.

Taken together, these findings indicate that HFD induced morphological changes in BAT together with transcriptional changes in inflammatory-, thermogenesis- and ECM-remodeling-related genes, while GDF15 selectively modulated the expression of inflammatory and mitochondrial genes.

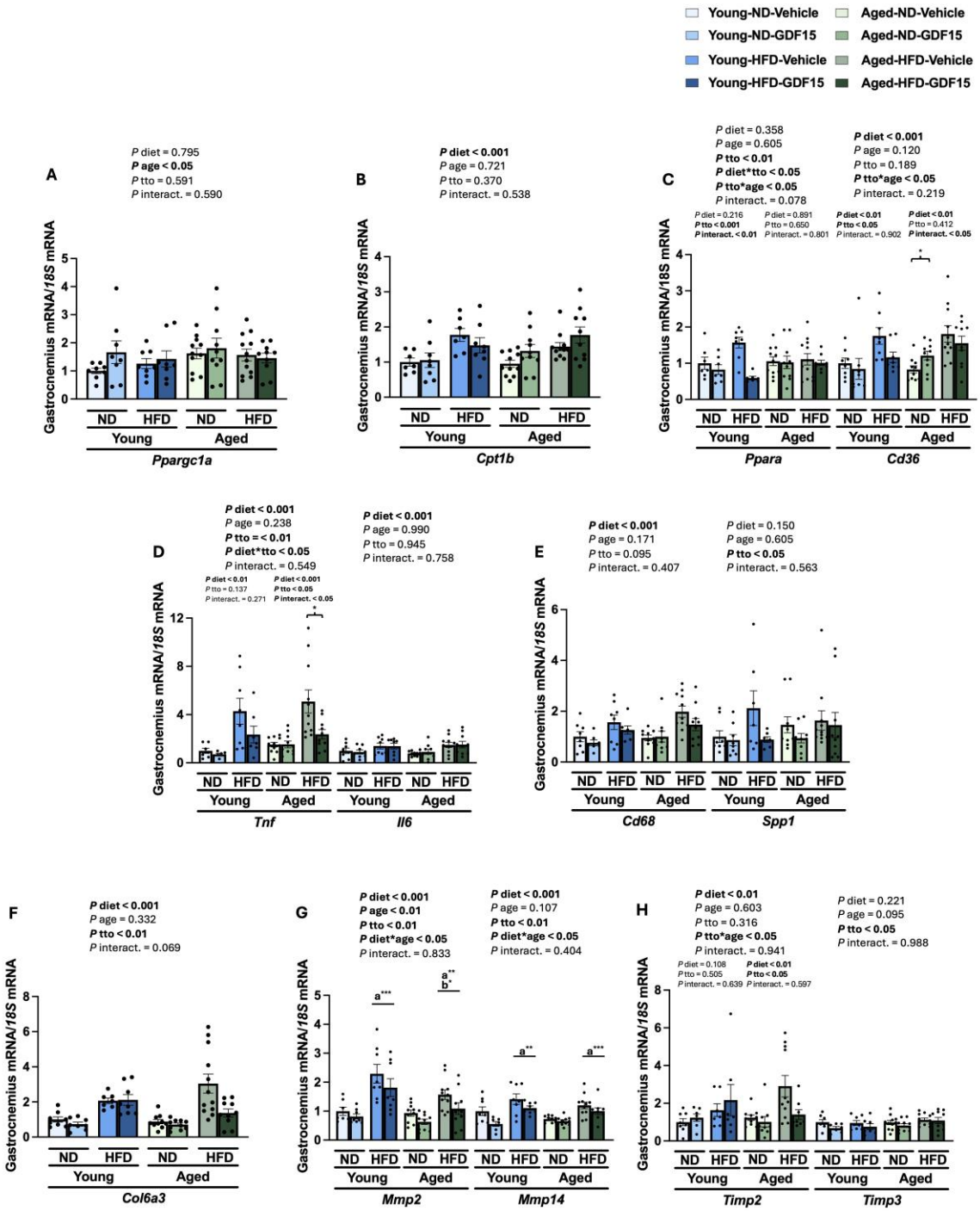


Figure 6. Gastrocnemius muscle gene expression. Relative mRNA expression of selected genes in gastrocnemius: **(A)** *Ppargc1a*; **(B)** *Cpt1b*; **(C)** *Ppara* and *Cd36*; **(D)** *Tnf* and *Il6*; **(E)** *Cd68* and *Spp1*; **(F)** *Col6a3*; **(G)** *Mmp2* and *Mmp14*; **(H)** *Timp2* and *Timp3.* Data are presented as the mean ± SEM. Exact sample sizes for each analysis are provided in Supplementary Table 3. Differences between groups were tested by three- or two-way ANOVA followed by Student's *t*-tests when necessary. *P* values displayed at the top of each graph correspond to three-way ANOVA results, whereas the additional *P* values shown below correspond to subsequent two-way ANOVA analyses performed when significant interactions were detected in the three-way ANOVA. Only significant partial interactions between factors were represented. The letters and asterisks indicate Student's *t*-test comparisons. a denotes HFD vs. ND comparisons within the same age group; b denotes young vs. old comparisons within the same type of diet. **P* < 0.05, ***P* < 0.01, ****P* < 0.001.

GDF15 treatment has limited effects on metabolic genes but induces broader changes in ECM-related gene expression in skeletal muscle

We next analyzed the gastrocnemius muscle to further characterize tissue-specific metabolic responses to HFD, aging and the effects of GDF15 treatment. Analysis of mitochondrial genes showed that *Ppargc1a* expression was not significantly affected by either diet or treatment (Fig. 6A). However, HFD broadly increased the expression of mitochondrial electron transport chain genes (Supplementary Fig. 8A). GDF15 reduced *Cox4i1* expression in young mice (Supplementary Fig. 8A).

Regarding lipid metabolism, HFD increased the mRNA expression of *Cpt1b* (Fig. 6B) and *Cd36* (involved in fatty acid uptake) (Fig. 6C), while *Ppara* expression remained unchanged (Fig. 6C). GDF15 treatment reduced *Ppara* and *Cd36* expression in young mice, as well as *Cd36* expression in aged ND-fed mice (Fig. 6C). In contrast, genes involved in glucose metabolism, including *Slc2a4, Foxo1* and *Nr4a1* were not significantly modulated by either diet or treatment (Supplementary Fig. 8B-C).

As expected, HFD feeding significantly increased the mRNA expression of several inflammatory markers, including *Tnf, Il6* and *Cd68* (Fig. 6D-E). GDF15 treatment significantly reduced *Tnf* expression in aged HFD-fed mice (Fig. 6D) and decreased *Spp1* expression across all experimental groups (Fig. 6E), indicating a reduction in the expression of inflammatory effect.

Finally, HFD induced transcriptional changes in ECM-related genes in muscle, as indicated by increased expression of *Col6a3* (Fig. 6F), *Mmp2, Mmp14* (Fig. 6G) and *Timp2* (Fig. 6H). Notably, GDF15 administration consistently reduced the expression of several ECM-related genes, including *Col6a3* (Fig. 6F), *Mmp2*, *Mmp14* (Fig. 6G) and *Timp3* (Fig. 6H) across all groups, as well as *Timp2* in aged mice (Fig. 6H).

Overall, HFD induced transcriptional changes consistent with a pro-inflammatory state accompanied by changes in the expression of ECM-related genes in gastrocnemius muscle, while lipid metabolism-related genes were selectively altered and glucose-related genes remained largely unchanged. GDF15 predominantly reduced the expression of inflammatory and ECM-related genes, with minimal effects on metabolism-related genes.

GDF15 reduces hepatic steatosis and differentially modulates inflammatory and ECM-related gene expression in the liver

Given the central role of the liver in systemic metabolism, we finally examined the hepatic responses to HFD and aging and the effects of GDF15 treatment. HFD feeding increased hepatic lipid accumulation, as evidenced by H&E staining and elevated TG content (Fig. 7A-B). Notably, this effect was significantly reduced by GDF15 treatment in young mice and in aged ND-fed mice (Fig. 7A-B). At the transcriptional level, HFD feeding significantly increased the mRNA expression of *Cd36* while reducing *Acaca*, indicating differential regulation of genes involved in lipid metabolism (Fig. 7C). *Ppara* expression was also significantly increased by HFD in young mice, although this effect was attenuated in aged mice (*P*=0.054) (Fig. 7C). GDF15 treatment did not modify *Cd36* or *Acaca* expression, despite reducing hepatic TG content, but significantly decreased *Ppara* expression in aged mice independently of diet.

HFD also increased the expression of genes related to hepatic inflammation, including *Tnf*, *Il6* and *Saa3,* as well as macrophage-associated genes such as *Cd68*, *Itgax* and *Spp1* (Fig. 7D-E). GDF15 treatment significantly reduced the expression of *Tnf* (Fig. 7D), *Cd68* and *Itgax* (Fig. 7E), indicating a reduction in the expression of inflammatory and macrophage-associated genes. The reduction in *Cd68* expression was age-dependent, being significant only in aged mice (Fig. 7E).

We next examined the expression of genes involved in hepatic mitochondrial regulation. Although HFD did not affect *Ppargc1a* expression, it increased the mRNA expression of *Sdhc* and *Cox4i1* in both young and aged mice, as well as *Atp5b* in young mice. *Ppargc1a* expression was upregulated in young ND-fed mice but downregulated in aged mice by GDF15 (Fig. 7F). This was accompanied by reduced expression of *Ndufa6*, *Sdhc, Uqcrb, Cox4i1* and *Atp5b* in aged mice (Fig. 7G). GDF15 treatment also tended to reduce the expression of these genes in young HFD-fed mice, although these changes only reached statistical significance for *Uqcrb* and *Atp5b* (Fig. 7G).

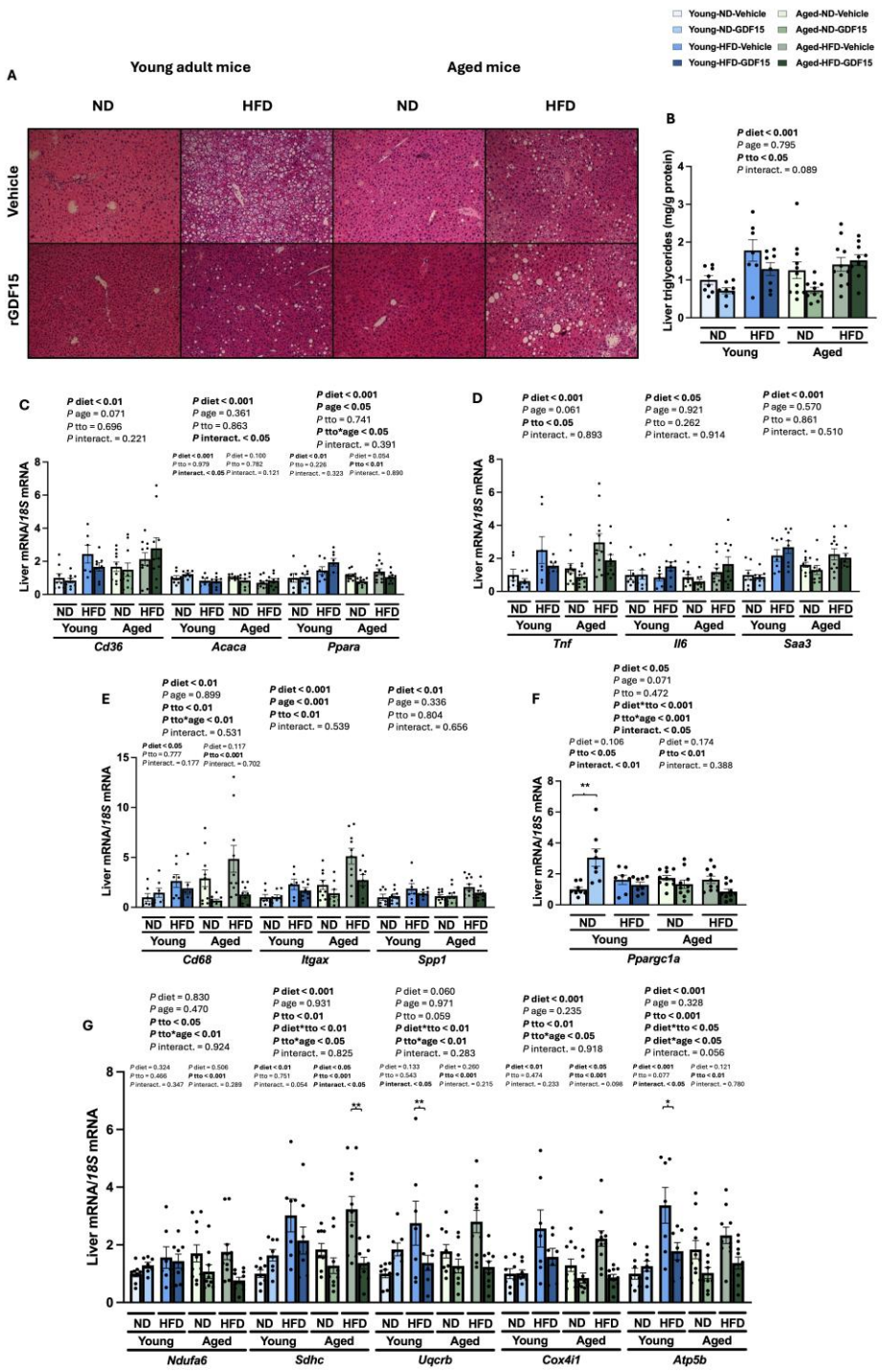


Figure 7. Hepatic steatosis and gene expression. (A) Hematoxylin and eosin staining of the liver (magnification ×200). **(B)** Liver triglycerides. Relative mRNA expression of selected genes in liver: **(C)** *Cd36*, *Acaca* and *Ppara*; **(D)** *Tnf, Il6* and *Saa3*; **(E)** *Cd68*, *Itgax* and *Spp1*; **(F)** *Ppargc1a*; **(G)** *Ndufa6, Sdhc, Uqcrb, Cox4i1* and *Atp5b*. Data are presented as the mean ± SEM. Exact sample sizes for each analysis are provided in Supplementary Table 3. Differences between groups were tested by three- or two-way ANOVA followed by Student's *t*-tests when necessary. *P* values displayed at the top of each graph correspond to three-way ANOVA results, whereas the additional *P* values shown below correspond to subsequent two-way ANOVA analyses performed when significant interactions were detected in the three-way ANOVA. Only significant partial interactions between factors were represented. The asterisks indicate Student's *t*-test comparisons. $*P < 0.05$, $**P < 0.01$.

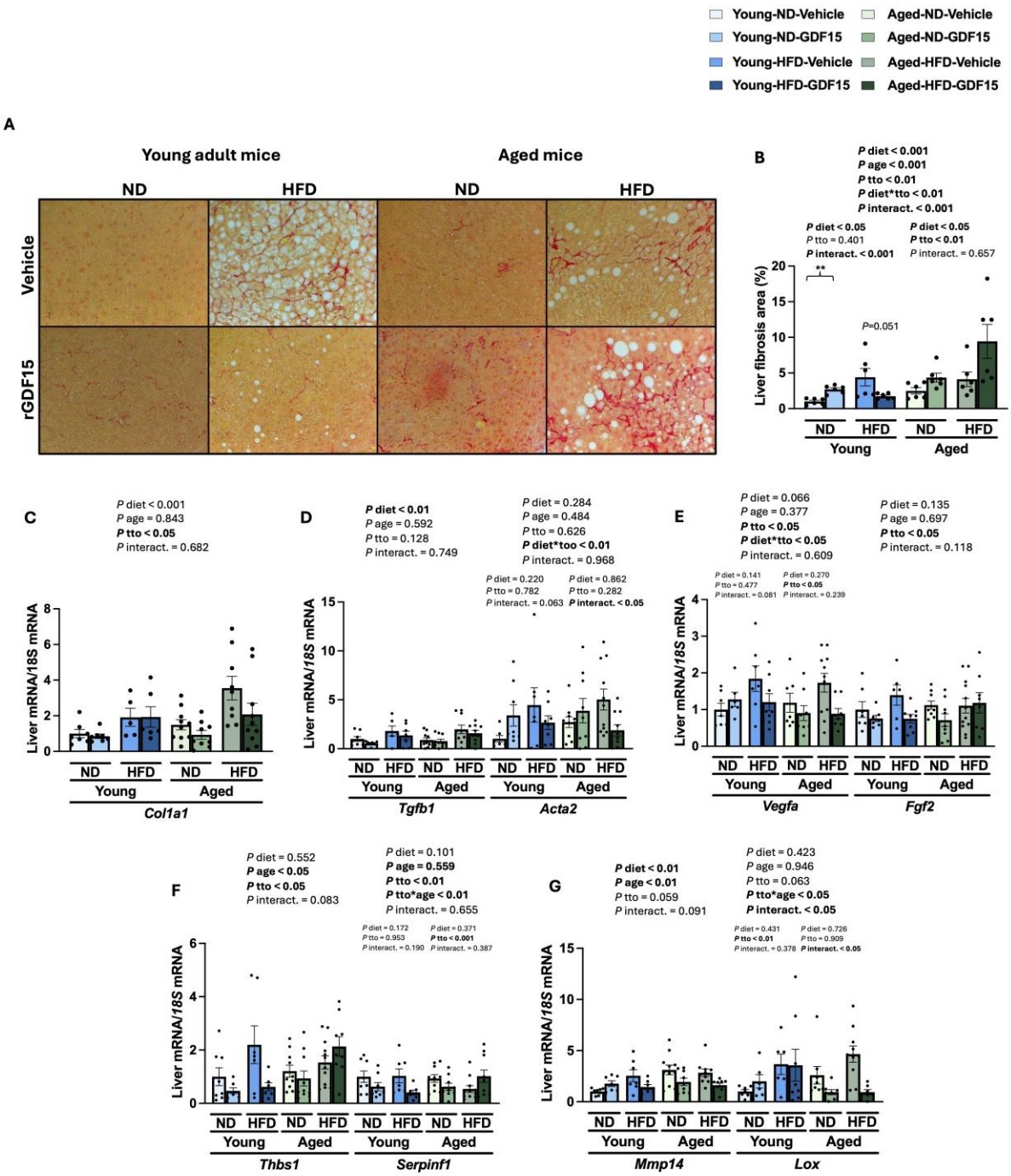


Figure 8. Hepatic fibrosis and extracellular matrix remodeling. (A) Sirius red staining of the liver (magnification ×200). Quantified **(B)** fibrosis area (%). Relative mRNA expression of selected genes in liver: **(C)** *Col1a1;* **(D)***Tgfb1 and Acta2;* **(E)** *Vegfa and Fgf2;* **(F)** *Thbs1 and Serpinf1;* ***(G)*** *Mmp14 and Lox.* Data are presented as the mean ± SEM. Exact sample sizes for each analysis are provided in Supplementary Table 3. Differences between groups were tested by three- or two-way ANOVA followed by Student's *t*-tests when necessary. *P* values displayed at the top of each graph correspond to three-way ANOVA results, whereas the additional *P* values shown below correspond to subsequent two-way ANOVA analyses performed when significant interactions were detected in the three-way ANOVA. Only significant partial interactions between factors were represented. The asterisks indicate Student's *t*-test comparisons. $^{**}P < 0.01$.

Finally, we assessed hepatic fibrosis and the expression of fibrosis and ECM-related genes. HFD increased collagen deposition (Fig. 8A-B) and upregulated the mRNA expression of *Col1a1* (Fig. 8C) and *Tgfb1* (Fig. 8D), a pro-fibrotic factor. GDF15 treatment increased fibrosis in young ND-fed and aged mice (Fig. 8A-B), despite decreased *Col1a1* expression (Fig. 8C), but without significantly affecting *Tgfb1* expression (Fig. 8D). *Acta2* expression, a marker of hepatic stellate cell activation, was not affected by diet or treatment alone, but showed a significant diet x treatment interaction in aged mice, with a trend toward increased expression in ND-fed mice and decreased expression in HFD-fed mice; however, individual comparisons did not reach statistical significance (Fig. 8E). In contrast, HFD did not induce broad changes in hepatic ECM-related genes, only inducing the expression of *Thbs1* (Fig. 8G). However, GDF15 significantly reduced the expression of several pro-angiogenic and ECM remodeling genes, including *Vegfa, Fgf2, Mmp14, Lox* and *Serpinf1* (Fig. 8E-G), with differential responses depending on the gene. *Fgf2* was consistently downregulated across all groups, with the exception of aged HFD-fed mice, whereas *Vegfa* and *Lox* were only reduced in aged mice (Fig. 8E-F) and *Serpinf1* was reduced in young mice (Fig. 8G). *Mmp14* expression decreased in young HFD-fed and aged mice (Fig. 8F). Moreover, GDF15 also tended to decrease *Thbs1* expression in young and aged HFD-fed mice (P=0.059) (Fig. 8G).

Altogether, these findings indicate that GDF15 reduced hepatic lipid accumulation and differentially modulated the hepatic expression of inflammatory- and ECM-related genes in an age- and diet-dependent manner. Notably, GDF15 increased hepatic collagen deposition in specific groups despite the absence of a pro-fibrotic transcriptional response, suggesting a potential context-dependent adverse effect that warrants further investigation.

Possible sex-specific modulation in GDF15-mediated responses

We performed an additional four-way ANOVA including sex, diet, treatment, and age to explore potential sex-dependent modulation of the observed effects. This analysis was conducted in an exploratory context to further assess whether sex influences transcriptional and metabolic responses across tissues. Given the subdivision of experimental groups across four factors, the resulting reduction in sample size per group limits statistical power to detect higher-order interactions. Therefore, the study was not designed or statistically powered to support definitive conclusions regarding sex-specific differences, and these analyses were not used for primary inference.

This analysis identified some sex-associated differences in gene expression across tissues. However, these effects were gene- and tissue-specific and did not converge on a consistent pattern across metabolic pathways. Interactions between sex and treatment were limited, and other interactions with more factors were observed only in isolated genes without reproducibility across tissues or functional pathways (Supplementary Table 2). To further explore potential sex-dependent metabolic responses, selected key metabolic outcomes were also analyzed separately in females and males (Supplementary Fig. 9). GDF15-induced weight loss was observed in both sexes, whereas some metabolic responses differed between them.

Therefore, these results should be interpreted as exploratory and hypothesis-generating. Overall, these findings suggest that sex may contribute to the modulation of transcriptional and metabolic responses to GDF15 in a context-dependent manner (Supplementary Fig. 9 and Supplementary Table 2).

DISCUSSION

GDF15 has emerged as a key stress-responsive cytokine involved in the regulation of energy balance, primarily through its effects on appetite suppression [17]. In preclinical models, GDF15 administration has been associated with reduced food intake and improvements in metabolic homeostasis [15]. However, the metabolic effects of GDF15 remain variable across studies, suggesting context-dependent responses. In the present study, we show that both diet and age influence the metabolic and tissue-specific responses to GDF15 treatment, revealing marked heterogeneity across experimental groups. This suggests that the metabolic actions of GDF15 are highly context-dependent, with both age and nutritional status shaping its systemic effects.

Consistent with previous studies, GDF15 treatment reduced body weight across all groups. This effect appeared more pronounced in HFD-fed and aged mice. In young mice, GDF15-induced weight loss was accompanied by reduced food intake, particularly under HFD conditions. In contrast, aged mice exhibited weight loss despite no significant changes in food intake. These findings suggest that the anorectic effects of GDF15 are modulated by both age and nutritional status and raise the possibility that mechanisms beyond appetite suppression may contribute to the systemic effects of GDF15. These observations are in accordance with previous studies reporting enhanced weight loss following GDF15 administration or overexpression in HFD-fed mice [24, 26], at least partly mediated through appetite suppression [9, 12]. The greater reduction in food intake in HFD-fed mice compared with ND-fed mice may reflect the ability

of GDF15 to reduce preference for HFD [39]. GDF15-mediated weight loss is often associated with reductions in fat mass [24, 30]. Herein, GDF15 showed a modest trend toward reducing total adiposity, as suggested by reductions in WAT depot weights, while significantly decreasing BAT, heart, and spleen weight. Moreover, liver weight also tended to decrease with GDF15, all of which may contribute to the reduction in total body weight. Consistent with previous reports, GDF15 did not significantly affect the weights of the gastrocnemius and soleus muscles.

Previous studies have demonstrated that reduced food intake alone does not fully explain GDF15-induced weight loss, and increased energy expenditure has been reported to contribute to its metabolic effects [28]. Although energy expenditure was not directly assessed, transcriptional analysis of BAT revealed that GDF15 increased *Ppargc1a* expression, without changes in *Ucp1* expression. This was accompanied by morphological changes, as GDF15 reduced lipid droplet accumulation, suggesting an attenuation of HFD-induced BAT whitening. Although some authors have found increased energy expenditure and BAT browning by GDF15 [24], our results are more consistent with reports showing no marked effect on *Ucp1* expression [26, 30]. Together, these findings suggest that GDF15 induced changes in BAT morphology and the expression of genes involved in mitochondrial regulation. These findings are compatible with the involvement of mechanisms other than canonical UCP1-dependent thermogenesis, although this could not be directly addressed in the present study.

At the systemic level, GDF15 treatment was associated with improved glucose tolerance and insulin sensitivity, reduced circulating TG, and increased the adiponectin/leptin ratio, consistent with improved metabolic homeostasis. Interestingly, these effects were observed across dietary and age conditions, despite differences in body weight loss between groups. This is in line with previous studies showing that GDF15 increases insulin action in several tissues independently of body weight and food intake changes [40]. Additionally, although GDF15 did not modulate the systemic inflammatory response induced by obesity and aging, it induced tissue-specific downregulation of inflammatory genes.

At the tissue level, both HFD and aging induced well-characterized morphological and molecular changes, including altered expression of genes related to inflammation, ECM remodeling, mitochondrial regulation, and lipid metabolism. HFD was the predominant factor driving broad morphological and transcriptional remodeling across tissues. GDF15 treatment induced selective effects in a tissue-, diet- and age-dependent manner, which may contribute to the systemic metabolic improvements observed.

The broadest transcriptional responses were observed in gastrocnemius muscle and liver, whereas adipose tissues showed more selective changes. However, all tissues exhibited GDF15-induced modulation of inflammatory gene expression. This response differed between tissues, with the liver showing greater downregulation of immune cell-associated genes, including *Tnf*, *Cd68* and *Itgax*, whereas gastrocnemius muscle and adipose tissues displayed a more general attenuation of inflammatory gene expression, reflected by reduced expression of mediators such as *Spp1*, *Saa3* and *Il6,* in tissue-, age-, and diet-dependent patterns.

The hepatic response to GDF15 was strongly age-dependent and, to a lesser extent, influenced by diet, with aged mice showing more widespread transcriptional changes, including reduced inflammatory, mitochondrial, and ECM-remodeling gene expression. In contrast, young mice exhibited more selective and diet-dependent effects, with GDF15 treatment being more effective in those fed a HFD. GDF15 significantly reduced hepatic TG content in young and aged ND-fed mice, indicating reduced hepatic steatosis. Notably, this effect was absent in aged HFD-fed mice, suggesting that hepatic lipid handling may depend more on metabolic flexibility rather than baseline lipid levels. Importantly, GDF15 treatment increased hepatic collagen deposition in young ND-fed and aged mice, indicating a potential context-dependent pro-fibrotic effect. This effect was observed despite reduced *Col1a1* expression in aged mice and the absence of alterations in the classical pro-fibrotic marker *Tgfb1*. Moreover, hepatic fibrosis increased in aged HFD-fed mice despite a tendency toward reduced *Acta2* expression, together with decreased *Vegfa, Mmp14* and *Lox* expression, whereas *Fgf2*, *Thbs1* and *Serpinf1* were selectively upregulated. This apparent dissociation between histological and transcriptional findings indicates that increased collagen deposition occurred despite the absence of a classical pro-fibrotic transcriptional profile, suggesting that additional mechanisms may contribute to fibrosis progression. These findings support a context-dependent effect of GDF15 on hepatic fibrosis [41]. Importantly, the histological evidence of increased collagen deposition should be considered when evaluating the therapeutic potential of GDF15-based interventions, as it raises the possibility of context-dependent adverse effects. Further studies are required to clarify the mechanisms underlying these observations and the long-term implications of GDF15-based interventions. Moreover, the observed downregulation of mitochondrial gene expression in aged groups may, in part, reflect the reduction in lipid availability following GDF15 treatment, and consequently decreased demand for oxidative

metabolism. However, this does not fully explain the changes observed in aged HFD-fed mice, where mitochondrial gene expression was reduced despite unchanged hepatic TG content, suggesting that additional mechanisms may contribute to these changes beyond differences in lipid substrate availability.

The downregulation of mitochondrial electron transport chain genes was largely restricted to the liver, whereas adipose tissues and gastrocnemius muscle showed minimal changes in these genes despite increased *Ppargc1a* expression in adipose depots. These findings further support tissue-specific and partial transcriptional responses to GDF15, rather than a uniform upregulation of genes involved in oxidative metabolism. In addition, gastrocnemius also showed a broad downregulation of ECM remodeling-related genes in response to GDF15, whereas eWAT exhibited more limited and age-dependent transcriptional changes. Although eWAT is a rodent-specific visceral fat depot without a direct anatomical counterpart in humans, it is widely used as a representative visceral adipose tissue depot in preclinical studies. Therefore, findings obtained in eWAT should be interpreted with caution when extrapolating to human visceral adipose tissue [42, 43].

Remarkably, the liver emerged as the tissue showing the most pronounced transcriptional response to GDF15, despite exhibiting the lowest diet-induced increase in *Gdf15* expression and no correlation between hepatic *Gdf15* mRNA levels and its circulating concentrations. This dissociation suggests that hepatic effects of GDF15 are primarily driven by endocrine signaling rather than local production. In contrast, eWAT showed a positive correlation between *Gdf15* expression and its circulating concentrations across all experimental conditions, supporting its described role as a major contributor to systemic GDF15 under obesogenic conditions [44]. Interestingly, BAT displayed the highest induction of *Gdf15* expression under HFD, and positive associations with GDF15 serum levels, particularly following GDF15 treatment, suggesting a context-dependent contribution of thermogenic adipose tissue. In obesity and aging, BAT undergoes a degenerative decline characterized by tissue inflammation [45]. Macrophage recruitment is a key driver of this decline, contributing to BAT whitening and impaired thermogenesis. Increased *Gdf15* expression in eWAT and BAT observed in our study might reflect excessive accumulation of macrophages within these tissues, which are the main immune cells expressing GDF15 [44]. Overall, circulating GDF15 appears to be differentially shaped by distinct metabolic tissues in a context-dependent manner, with adipose tissue depots, particularly BAT and eWAT, potentially representing major contributors, whereas liver and gastrocnemius appear to play a more limited role in obesity conditions.

Finally, although *Gfral* expression has been usually restricted to the brainstem, with only limited evidence of low peripheral expression [13, 14], one of our qPCR assays consistently detected very low *Gfral* expression in liver and gastrocnemius muscle. This suggests that *Gfral* may be expressed at very low levels in some peripheral tissues. Therefore, additional studies will be required to confirm *Gfral* expression in peripheral tissues and to determine whether very low peripheral *Gfral* expression has any biological relevance.

Our study has several limitations that should be acknowledged. First, pair-fed control groups were not included; therefore, we cannot determine to what extent the observed metabolic and transcriptional changes are attributable to reduced energy intake and body weight loss rather than direct tissue-specific effects of GDF15. Second, indirect calorimetry was not performed. Consequently, energy expenditure could not be directly measured, limiting our ability to determine its contribution to the observed changes in body weight. Third, whole-body composition was not directly measured; therefore, conclusions regarding fat and lean mass should be interpreted with caution. Fourth, while we performed a comprehensive analysis of transcriptional and histological changes across multiple tissues, protein-level and functional validation of the affected pathways was not carried out. Therefore, our conclusions are primarily based on gene expression and histological analyses. Fifth, given the large number of genes, tissues, and statistical comparisons assessed, the possibility of false-positive findings cannot be completely excluded. Gene expression analyses were therefore considered exploratory. Finally, while our findings suggest low levels of peripheral *Gfral* expression, definitive validation of its functional relevance in peripheral tissues will require further investigation. Despite these limitations, the experimental design, including different tissues, dietary conditions, age groups, and sex, provides a robust framework to assess the systemic and tissue-specific responses to GDF15 treatment.

CONCLUSION

GDF15 induces robust reductions in body weight, with diet- and age-dependent effects. Despite differences in body weight loss across groups and heterogeneous tissue-specific responses, GDF15 treatment was associated with consistent improvements in systemic metabolic homeostasis, including improved glucose tolerance, reduced insulin resistance, and lower circulating TG levels, which were impaired by HFD and aging (Fig. 9). Among tissues, the liver showed the strongest transcriptional response, including attenuation of hepatic steatosis, whereas BAT also exhibited marked

morphological and transcriptional changes, including reduced BAT whitening. Gastrocnemius muscle responses were more conserved across diet and age, whereas WAT displayed more restricted changes, although all tissues exhibited some degree of downregulation of inflammatory gene expression. Notably, GDF15 induced broader transcriptional changes in tissues from aged mice. In addition, exploratory analyses suggest that sex may also contribute to variability in GDF15 responses. Overall, our study shows that GDF15 effects are not only influenced by diet conditions, but are also modulated by age, highlighting the importance of considering age when evaluating the therapeutic potential of GDF15-based interventions.

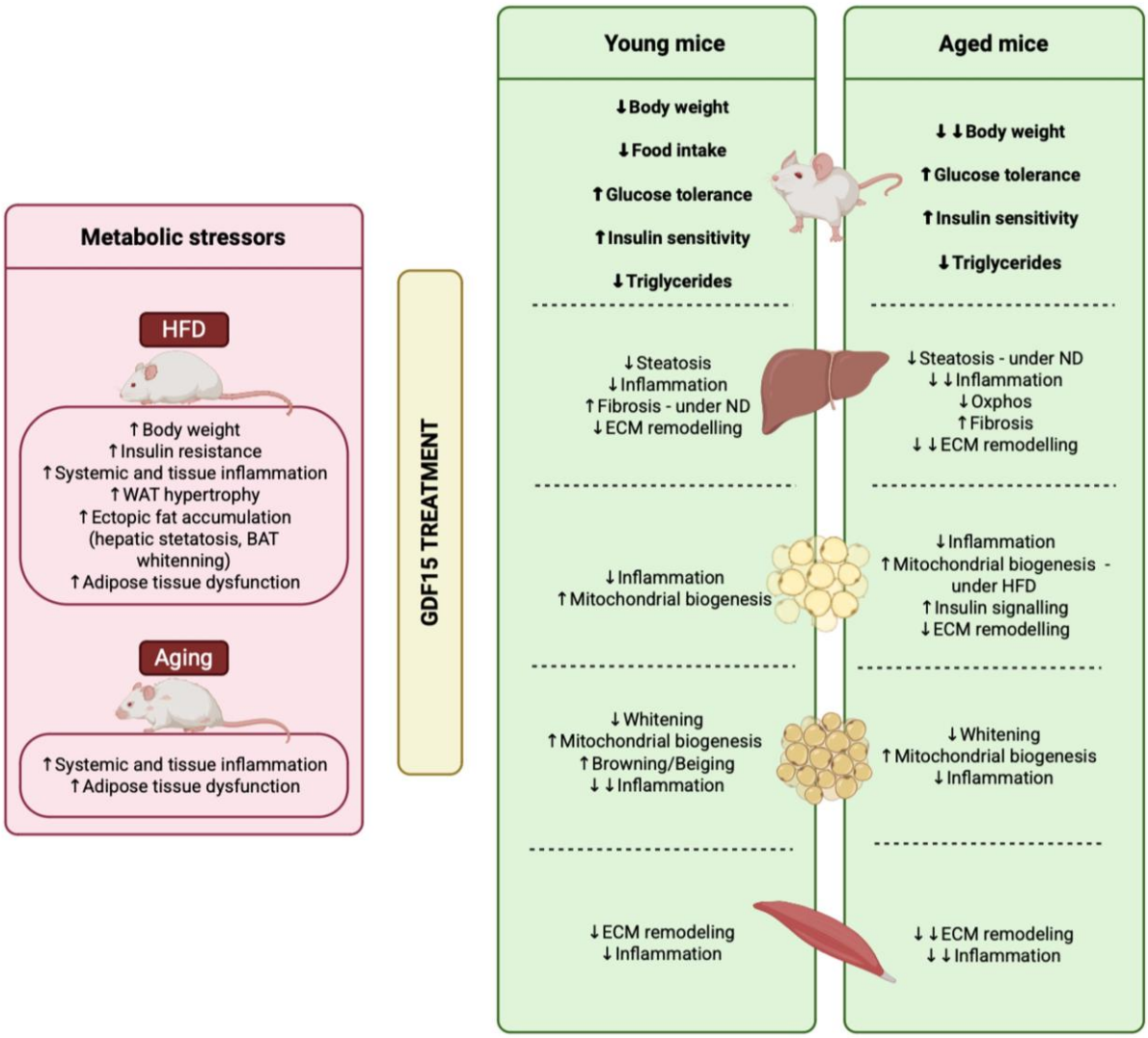


Figure 9. Summary of the effects of GDF15 according to diet and age. HFD and aging induce metabolic alterations that are improved by GDF15 treatment, with aging as the major determinant of the response. ECM, extracellular matrix; GDF15, growth differentiation factor 15; HFD, high-fat diet; TG, triglycerides. ↑/↓ indicates significant effect, ↑↑/↓↓ indicates greater magnitude of change.

Acknowledgments

This study was funded by Plan Estatal I+D+I from the Spanish Instituto de Salud Carlos III–Subdirección General de Evaluación y Fomento de la Investigación–cofunded by European Union (grants number PI20/00080, PI23/00208, PI24/01147 and PI25/00528) and CIBEROBN, ISCIII, Spain; Dpt. of Health 58/2021, Gobierno de Navarra-FEDER, Spain. The funders had no role in study design, decision to publish, or preparation of the manuscript.

Author Contributions

G.F. and J.G.-A. designed the study and obtained the funds. L.S.-G., G.F. and J.G.-A. analyzed and interpreted

the data. L.S.-G. and J.G.-A. drafted the manuscript. L.S.-G., V.C., B.R., M.A.-A, A.R., S.B., G.F., and J.G.-A. provided study materials or performed experiments. V.C., B.R., M.A.-A, A.R., S.B., G.F., and J.G.-A. critically revised the article for important intellectual content. All authors read and approved the final version of the article. L.S.-G., G.F. and J.G.-A. are the guarantors of this work and, as such, had full access to all the data in the study and take responsibility for the integrity of the data and the accuracy of the data analysis.

Conflict of interests

G.F. declares payment of honoraria for lectures from Novo Nordisk as Member of the OPEN Spain Initiative as well as payment of honoraria for attendance to Advisory Boards from Lilly, Novo Nordisk, Regeneron, AstraZeneca and Boehringer Ingelheim. The other authors declared no conflict of interest.

Supplementary Materials

The Supplementary data can be found online at: www.aginganddisease.org/EN/10.14336/AD.2026.0702.

References

[1] Carbone F, Després JP, Ioannidis JPA, Neeland IJ, Garruti G, Busetto L, et al. (2025). Bridging the gap in obesity research: A consensus statement from the European Society for Clinical Investigation. Eur J Clin Invest, 55:e70059.

[2] Perdomo CM, Cohen RV, Sumithran P, Clément K, Frühbeck G (2023). Contemporary medical, device, and surgical therapies for obesity in adults. Lancet, 401:1116-1130.

[3] Tian T, Liu M, Little PJ, Strijdom H, Weng J, Xu S (2025). Emerging roles of GDF15 in metabolic and cardiovascular diseases. Research (Wash D C), 8:0832.

[4] Li J, Hu X, Xie Z, Li J, Huang C, Huang Y (2024). Overview of growth differentiation factor 15 (GDF15) in metabolic diseases. Biomed Pharmacother, 176:116809.

[5] Zhang J, Sun J, Li J, Xia H (2024). Targeting the GDF15 signalling for obesity treatment: recent advances and emerging challenges. J Cell Mol Med, 28:e70251.

[6] Keipert S, Ost M (2021). Stress-induced FGF21 and GDF15 in obesity and obesity resistance. Trends Endocrinol Metab, 32:904-915.

[7] Kim KH, Lee MS (2021). GDF15 as a central mediator for integrated stress response and a promising therapeutic molecule for metabolic disorders and NASH. Biochim Biophys Acta Gen Subj, 1865:129834.

[8] Picard M, Murugan NJ (2025). The energy resistance principle. Cell Metab, 37:2107-2127.

[9] Yang L, Chang CC, Sun Z, Madsen D, Zhu H, Padkjær SB, et al. (2017). GFRAL is the receptor for GDF15 and is required for the anti-obesity effects of the ligand. Nat Med, 23:1158-1166.

[10] Mullican SE, Lin-Schmidt X, Chin CN, Chavez JA, Furman JL, Armstrong AA, et al. (2017). GFRAL is the receptor for GDF15 and the ligand promotes weight loss in mice and nonhuman primates. Nat Med, 23:1150-1157.

[11] Emmerson PJ, Wang F, Du Y, Liu Q, Pickard RT, Gonciarz MD, et al. (2017). The metabolic effects of GDF15 are mediated by the orphan receptor GFRAL. Nat Med, 23:1215-1219.

[12] Hsu JY, Crawley S, Chen M, Ayupova DA, Lindhout DA, Higbee J, et al. (2017). Non-homeostatic body weight regulation through a brainstem-restricted receptor for GDF15. Nature, 550:255-259.

[13] Fichtner K, Kalwa H, Lin MM, Gong Y, Müglitz A, Kluge M, et al. (2024). GFRAL is widely distributed in the brain and peripheral tissues of mice. Nutrients, 16:734.

[14] Hes C, Gui LT, Bay A, Alvarez F, Katz P, Paul T, et al. (2025). GDNF family receptor alpha-like (GFRAL) expression is restricted to the caudal brainstem. Mol Metab, 91:102070.

[15] Asrih M, Wei S, Nguyen TT, Yi HS, Ryu D, Gariani K (2023). Overview of growth differentiation factor 15 in metabolic syndrome. J Cell Mol Med, 27:1157-1167.

[16] Xiong Y, Walker K, Min X, Hale C, Tran T, Komorowski R, et al. (2017). Long-acting MIC-1/GDF15 molecules to treat obesity: Evidence from mice to monkeys. Sci Transl Med, 9:eaan8732.

[17] Patel S, Alvarez-Guaita A, Melvin A, Rimmington D, Dattilo A, Miedzybrodzka EL, et al. (2019). GDF15 provides an endocrine signal of nutritional stress in mice and humans. Cell Metab, 29:707-718.e708.

[18] Salmón-Gómez L, Catalán V, Ramírez B, Aguas-Ayesa M, Rodríguez A, Becerril S, et al. (2026). Different association of GDF15 and FGF21 with glycemic status and aging in the context of obesity. Geroscience, 48:2931-2944.

[19] Salmón-Gómez L, Catalán V, Ramírez B, Aguas-Ayesa M, Rodríguez A, Becerril S, et al. (2025). Differential effects of bariatric surgery on circulating GDF15 and FGF21 levels: Implications for glycemic status and weight loss outcomes. Eur J Clin Invest, 55:e70069.

[20] Chen J, Kastroll J, Bello FM, Pangburn MM, Murali A, Smith PM, et al. (2025). Skeletal muscle mitochondrial dysfunction is associated with increased Gdf15 expression and circulating GDF15 levels in aged mice. Sci Rep, 15:8101.

[21] Cardoso AL, Fernandes A, Aguilar-Pimentel JA, de Angelis MH, Guedes JR, Brito MA, et al. (2018). Towards frailty biomarkers: Candidates from genes and pathways regulated in aging and age-related diseases. Ageing Res Rev, 47:214-277.

[22] Moon JS, Goeminne LJE, Kim JT, Tian JW, Kim SH, Nga HT, et al. (2020). Growth differentiation factor 15 protects against the aging-mediated systemic inflammatory response in humans and mice. Aging Cell, 19:e13195.

[23] Tsai VW, Macia L, Johnen H, Kuffner T, Manadhar R, Jørgensen SB, et al. (2013). TGF-b superfamily cytokine MIC-1/GDF15 is a physiological appetite and body weight regulator. PLoS One, 8:e55174.

[24] Tsai VW, Zhang HP, Manandhar R, Lee-Ng KKM, Lebhar H, Marquis CP, et al. (2018). Treatment with the TGF-b superfamily cytokine MIC-1/GDF15 reduces the adiposity and corrects the metabolic dysfunction of mice with diet-induced obesity. Int J Obes (Lond), 42:561-571.

[25] Tran T, Yang J, Gardner J, Xiong Y (2018). GDF15 deficiency promotes high fat diet-induced obesity in mice. PLoS One, 13:e0201584.

[26] Macia L, Tsai VW, Nguyen AD, Johnen H, Kuffner T, Shi YC, et al. (2012). Macrophage inhibitory cytokine 1 (MIC-1/GDF15) decreases food intake, body weight and improves glucose tolerance in mice on normal & obesogenic diets. PLoS One, 7:e34868.

[27] Johnen H, Lin S, Kuffner T, Brown DA, Tsai VW, Bauskin AR, et al. (2007). Tumor-induced anorexia and weight loss are mediated by the TGF-beta superfamily cytokine MIC-1. Nat Med, 13:1333-1340.

[28] Wang D, Townsend LK, DesOrmeaux GJ, Frangos SM, Batchuluun B, Dumont L, et al. (2023). GDF15 promotes weight loss by enhancing energy expenditure in muscle. Nature, 619:143-150.

[29] Chung HK, Ryu D, Kim KS, Chang JY, Kim YK, Yi HS, et al. (2017). Growth differentiation factor 15 is a myomitokine governing systemic energy homeostasis. J Cell Biol, 216:149-165.

[30] Chrysovergis K, Wang X, Kosak J, Lee SH, Kim JS, Foley JF, et al. (2014). NAG-1/GDF-15 prevents obesity by increasing thermogenesis, lipolysis and oxidative metabolism. Int J Obes (Lond), 38:1555-1564.

[31] Jeromson S, Akcan M, Baranowski B, Arbeau M, Bellucci A, Wright DC (2024). Daily GDF15 treatment has sex-specific effects on body weight and food intake and does not enhance the effects of voluntary physical activity in mice. J Physiol, 602:6813-6826.

[32] Wang X, Chrysovergis K, Kosak J, Kissling G, Streicker M, Moser G, et al. (2014). hNAG-1 increases lifespan by regulating energy metabolism and insulin/IGF-1/mTOR signaling. Aging (Albany NY), 6:690-704.

[33] Kim JM, Kosak JP, Kim JK, Kissling G, Germolec DR, Zeldin DC, et al. (2013). NAG-1/GDF15 transgenic mouse has less white adipose tissue and a reduced inflammatory response. Mediators Inflamm, 2013:641851.

[34] Becerril S, Rodríguez A, Catalán V, Sáinz N, Ramírez B, Collantes M, et al. (2010). Deletion of inducible nitric-oxide synthase in leptin-deficient mice improves brown adipose tissue function. PLoS One, 5:e10962.

[35] Becerril S, Rodríguez A, Catalán V, Méndez-Giménez L, Ramírez B, Sáinz N, et al. (2018). Targeted disruption of the iNOS gene improves adipose tissue inflammation and fibrosis in leptin-deficient ob/ob mice: role of tenascin C. Int J Obes (Lond), 42:1458-1470.

[36] Catalán V, Gómez-Ambrosi J, Rodríguez A, Silva C, Rotellar F, Gil MJ, et al. (2008). Expression of caveolin-1 in human adipose tissue is upregulated in obesity and obesity-associated type 2 diabetes mellitus and related to inflammation. Clin Endocrinol (Oxf), 68:213-219.

[37] Catalán V, Gómez-Ambrosi J, Rotellar F, Silva C, Rodríguez A, Salvador J, et al. (2007). Validation of endogenous control genes in human adipose tissue: relevance to obesity and obesity-associated type 2 diabetes mellitus. Horm Metab Res, 39:495-500.

[38] Siddiqui JA, Pothuraju R, Khan P, Sharma G, Muniyan S, Seshacharyulu P, et al. (2022). Pathophysiological role of growth differentiation factor 15 (GDF15) in obesity, cancer, and cachexia. Cytokine Growth Factor Rev, 64:71-83.

[39] Miyake M, Zhang J, Yasue A, Hisanaga S, Tsugawa K, Sakaue H, et al. (2021). Integrated stress response regulates GDF15 secretion from adipocytes, preferentially suppresses appetite for a high-fat diet and improves obesity. iScience, 24:103448.

[40] Sjøberg KA, Sigvardsen CM, Alvarado-Diaz A, Andersen NR, Larance M, Seeley RJ, et al. (2023). GDF15 increases insulin action in the liver and adipose tissue via a β-adrenergic receptor-mediated mechanism. Cell Metab, 35:1327-1340.e1325.

[41] Sawant H, Borthakur A (2025). Disease-specific novel role of growth differentiation factor 15 in organ fibrosis. Int J Mol Sci, 26:5713.

[42] Chusyd DE, Wang D, Huffman DM, Nagy TR (2016). Relationships between rodent white adipose fat pads and human white adipose fat depots. Front Nutr, 3:10.

[43] Börgeson E, Boucher J, Hagberg CE (2022). Of mice and men: pinpointing species differences in adipose tissue biology. Front Cell Dev Biol, 10:1003118.

[44] L'Homme L, Sermikli BP, Haas JT, Fleury S, Quemener S, Guinot V, et al. (2024). Adipose tissue macrophage infiltration and hepatocyte stress increase GDF-15 throughout development of obesity to MASH. Nat Commun, 15:7173.

[45] Jaeckstein MY, Fischer AW, Rissiek B, Staehler T, Heine M, Behrens J, et al. (2025). Purinergic adipocyte-macrophage crosstalk promotes degeneration of thermogenic brown adipose tissue. EMBO Rep, 26:6460-6493.